Eur Biophys J (1998) 27: 9–17

ARTICLE

Chun-Min Lo · Michael Glogauer · Marisa Rossi
Jack Ferrier

Cell-substrate separation: effect of applied force and temperature

Received: 20 June 1997 / Accepted: 24 August 1997

Abstract We measure the change in cell-substrate separation in response to an upward force by combining two relatively new techniques, Electric Cell-substrate Impedance Sensing (ECIS) to measure average cell-substrate separation, and collagen-coated magnetic beads to apply force to the top (dorsal) surface of cells. The collagen-coated ferric oxide beads attach to integrin receptors in the dorsal surfaces of osteoblastlike ROS 17/2.8 cells. Magnetic force is controlled by the position and the number of permanent magnets, applying an average 320 or 560 pN per cell. Comparing model calculations with experimental impedance data, the junctional resistivity of the cell layer and the average distance between the lower (ventral) cell surface and substrate can be determined. The ECIS analysis shows that these forces produce an increase in the distance between the ventral cell surface and the substrate that is in the range of 10 to 25%. At temperatures of 4°, 22° and 37 °C, the measured cell surface-substrate distances without magnetic beads are 84 ± 4, 45 ± 2 and 38 ± 2 nm. The force-induced changes at 22° are 11 ± 3 and 21 ± 3 nm for 320 and 560 pN, and at 37° they are 5 ± 2 and 9 ± 2 nm. The resulting cell-substrate spring constants at 22° and 37° are thus about 28 and 63 pN nm^{-1} (dyne cm^{-1}). Using a reasonable range for the number for individual integrin-ligand adhesion bonds gives a range for the spring constant of the individual adhesion bond of from about 10^{-3} to 10^{-1} pN nm^{-1}. These data also provide evidence that the number of adhesion bonds per cell increases with temperature.

Key words Cell adhesion · Spring constant · ECIS · Applied force · Integrins

C.-M. Lo · M. Glogauer · M. Rossi · J. Ferrier (✉)
Medical Research Council Group in Periodontal Physiology,
4384 Medical Sciences Building,
University of Toronto, Toronto, Ontario M5S 1A8, Canada
(e-mail: j.ferrier@utoronto.ca)

Introduction

Adhesion plays an important role in the movement, proliferation and differentiation of cells, and in tissue development and wound healing (Ingber 1990; Hynes and Lander 1992; Lauffenburger and Horwitz 1996). Cell attachment to extracellular molecules is mediated by the integrin family of receptors (Hynes 1987, 1992; Gumbiner 1996). The dynamics of integrin-ligand binding and the effect on cell-substrate adhesion have been studied through adhesion measurements and mathematical modeling (Bell 1978; Hammer and Lauffenburger 1987; Dembo et al. 1988; Lotz et al. 1989; Ward and Hammer 1993; Ward et al. 1994, 1995), but many physical properties of the integrin-ligand complex have not been determined.

Adhesion and separation between cell and substrate results from the interplay between nonspecific repulsion and specific bonding (Bell et al. 1984; Israelachvili and Wennerström 1996). Interference reflection microscopy shows a variable separation of from 10 to 100 nm between the ventral surface of adherent fibroblasts and the substrate (Izzard and Lochner 1976, 1980), depending on the degree of aggregation of adhesion bonds within a given area (Lotz et al. 1989; Ward and Hammer 1993).

The cell-substrate separation distance (h) also depends on the force (F) that the adhesion bonds experience; the relation between h and F can be described in terms of a spring constant, $k = F/\Delta h$. The main objective of this study was to measure the overall spring constant for cell-substrate adhesion, and from that to estimate the spring constant for individual integrin-ligand bonds. Theoretical treatments of cell-substrate adhesion show that the spring constant plays an important role in determining the force required to break the adhesion bond (Bell et al. 1984; Ward and Hammer 1993) and the rate at which adhesion bonds break when under stress (Ward et al. 1994, 1995). This is because a force, F, applied to a bond with a spring constant k_{bond}, can increase the potential energy in the bond by $F \times \Delta h = F^2/k_{bond}$, and this energy can contribute directly to breaking the adhesion bond. A wide range of val-

ues for k_{bond} have been obtained via theoretical arguments (Bell et al. 1984; Ward and Hammer 1993), but there have been no direct measurements of this key parameter. The effect of temperature on cell-substrate contact also provides important insights into the adhesion mechanisms (Ward and Hammer 1993; Lotz et al. 1989), so in addition to the effect of applied force, we studied the effect of temperature on the average cell-substrate separation.

Electric Cell-substrate Impedance Sensing (ECIS) has recently been developed to measure cell motion and morphology in tissue culture (Giaever and Keese 1984, 1986, 1993a; Lo et al. 1993). In the present investigation, we measure the impedance of an electrode blanketed with a confluent layer of osteoblasts. By comparing the impedance as a function of frequency with a model calculation, the junctional resistance of the cell layer and the average distance between the ventral cell surface and substrate can be determined (Giaever and Keese 1991, 1993b; Lo et al. 1995).

We apply an upward force on our cells by using a permanent magnet to attract collagen-coated ferric oxide beads that are attached to the upper (dorsal) cell surface via integrin receptors. This method of applying linear force to cell surfaces has recently been developed and quantified (Glogauer et al. 1995, 1997). Previously, magnetic beads have been used to apply torque to points on a cell surface, via the application of a magnetic field that produces a torque on the beads (Wang et al. 1993; Wang and Ingber 1995). Force application via magnetic beads has also been used to study the viscoelastic properties of cytoplasm (Crick and Hughes 1950; Hiramoto 1969) and the force-velocity relationship for actin filaments (Tregear et al. 1993). Other methods previously used to apply force to entire cells include fluid flow (Frangos et al. 1996), stretching of the substrate (Mikuni-Takagaki et al. 1996), touching by glass micropippete (Sanderson et al. 1990; Xia and Ferrier 1992), and hypotonic extracellular medium (Leijendekker et al. 1996). The method used here is the only one that can target a force (rather than a torque) directly to the integrin receptors on a cell surface. An upward force applied via this method to the dorsal surface will be transmitted via the cytoskeleton to the adhesion molecules that link integrin receptors on the lower (ventral) surface of the cell to the substrate.

Materials and methods

Cell culture

Rat osteosarcoma cells (ROS 17/2.8) were cultured at 37 °C and 5% CO_2 in α-minimal essential medium (α-MEM) with 10% heat-inactivated fetal bovine serum (FBS) (Flow Laboratories, Maclean, VA) and antibiotic (170 μg/ml penicillin V, 100 μg/ml gentamycin sulfate, and 1 μg/ml amphotericin; Sigma Chemical, St. Louis, MO). These cells have many osteoblast-like properties (Majeska and Rodan 1982; Ferrier et al. 1987, 1990), and have a hemispherical morphology. Twenty-four hours after inoculating cells into electrode-containing dishes at 10^5 cells cm^{-2}, the normal medium was replaced by α-MEM without bicarbonate and with 25 mM HEPES buffer, and 10% FBS. We used an incubator without CO_2 and a refrigerator as 37° and 4 °C environments respectively, and the room temperature was about 22 °C. Before taking data we waited at least 30 minutes after changing the temperature.

Impedance measurements and cell-substrate separation

Electrode arrays, relay bank, lock-in amplifier and software for the ECIS measurement were obtained from Applied BioPhysics (Troy, NY). Each electrode array consists of five wells, 10 mm in height and 50 mm^2 in area; each well contains a 250 μm diameter gold electrode and a much larger gold counter electrode. The large electrode and one of the small electrodes are connected via the relay bank to a phase-sensitive lock-in amplifier, and AC current is applied through a 1 MΩ resistor to the electrodes (Fig. 1) at frequencies from 22 Hz to 90 kHz (Giaever and Keese 1984, 1986, 1991, 1993a, 1993b; Lo et al. 1993). There are two mathematical models for the frequency scan data measured by ECIS: one for cells with lower junctional resistance such as fibroblasts and endothelial cells, and the other for cells with higher junctional resistance such as epithelial cells (Lo et al. 1995). For the osteoblastlike cells studied in this paper, we use the simpler model with two adjustable parameters, α ($=r_c(\rho/h)^{1/2}$) and R_b, to fit the experiment data:

$$\frac{1}{Z_c} = \frac{1}{Z_n}\left(\frac{Z_n}{Z_n + Z_m} + \frac{\dfrac{Z_m}{Z_n + Z_m}}{\dfrac{\gamma r_c}{2}\dfrac{I_0(\gamma r_c)}{I_1(\gamma r_c)} + R_b\left(\dfrac{1}{Z_n} + \dfrac{1}{Z_m}\right)} \right), \quad (1)$$

where Z_c (GΩ μm^2) is specific impedance (per unit area) of the cell-covered electrode, Z_n (GΩ μm^2) is specific impedance of the cell-free electrode, Z_m (GΩ μm^2) is specific impedance through both ventral and dorsal cell membranes, r_c (μm) is cell radius, R_b (GΩ μm^2) is junctional resistance between adjacent cells over a unit cell area, I_0 and I_1 are modified Bessel functions of the first kind in order 0 and 1, and

$$\gamma r_c = r_c \sqrt{\frac{\rho}{h}\left(\frac{1}{Z_n} + \frac{1}{Z_m}\right)} = \alpha \sqrt{\left(\frac{1}{Z_n} + \frac{1}{Z_m}\right)}, \quad (2)$$

$$Z_n = S[R_n + (1/\mathrm{i}\,2\pi f C_n)], \quad (3)$$

$$Z_m = 2[(1/R_m) + (\mathrm{i}\,2\pi f C_m)]^{-1}, \quad (4)$$

where ρ (Ω mm) is resistivity of the cell culture medium, h (nm) is average separation between the ventral cell surface and the substrate, S (μm^2) is electrode area, R_n (GΩ) is measured resistance of the cell-free electrode, f (hz) is frequency of the AC signal, C_n (pF) is measured capacitance of the cell-free electrode, R_m (GΩ μm^2) is specific

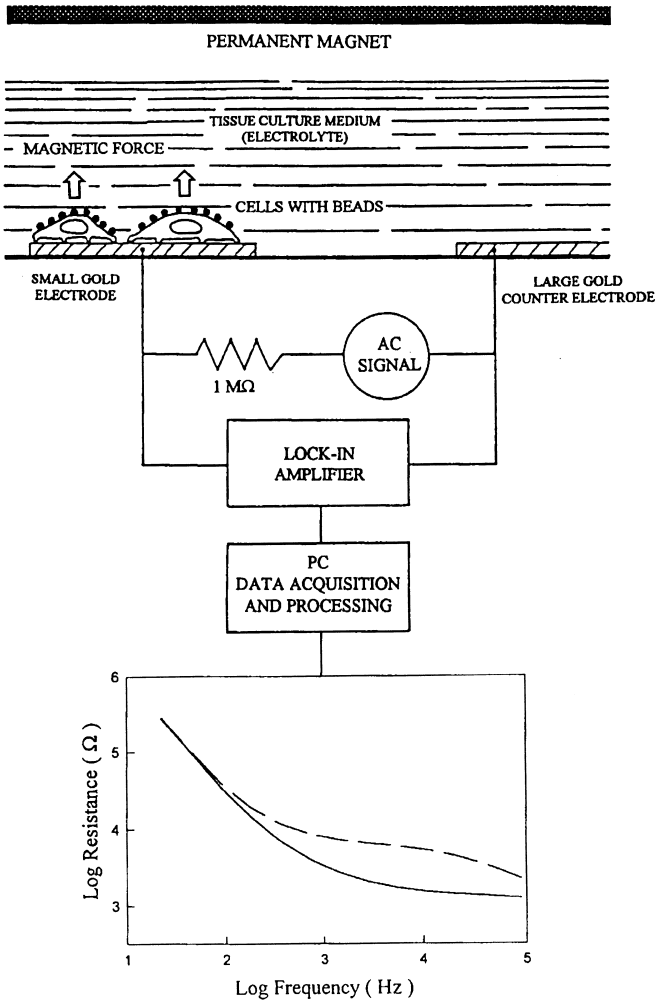

Fig. 1 A schematic of the experimental setup. The 1 MΩ series resistance provides a current source that makes the measured in-phase voltage proportional to resistance and the out-of-phase voltage proportional to reactance. The AC current delivered to the electrodes is kept at an amplitude of 1.2 μA or lower, which keeps the voltage drop across the cell layer below 7 mV. Collagen-coated beads are attached to integrin receptors in the dorsal surface of the cells and attracted by a permanent magnet

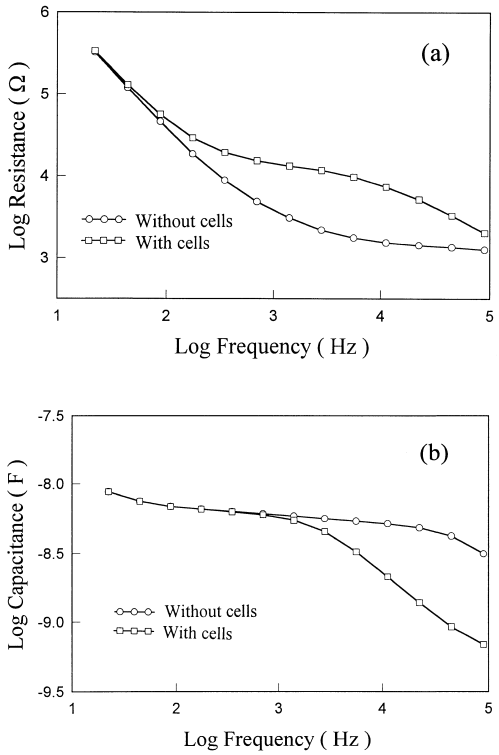

Fig. 2 **a** Resistance and **b** capacitance as a function of frequency obtained from a frequency scan measurement of an electrode with and without a monolayer of cells

resistance of the cell membrane, and C_m (pF μm^{-2}) is specific capacitance of the cell membrane.

The specific impedance of the cell-free electrode, Z_n, is interpreted as a resistor and a capacitor in series as shown in Eq. (3); R_n and C_n are based on the in-phase and out-of-phase data obtained from the lock-in amplifier at different frequencies. We also assume that the specific resistance and capacitance of the cell membrane, R_m and C_m, are 100 GΩ μm^2 (10^3 Ω cm^2) and 0.02 pF μm^{-2} (2 μF cm^{-2}) respectively, and that the specific impedance of the cell membrane can be calculated as a resistor and a capacitor in parallel as shown in Eq. (4). The factor 2 in Eq. (4) is the additive impedance of ventral and dorsal membranes in series. Both the in-phase and out-of-phase (resistive and reactive) components of the voltage signal from the lock-in amplifier are fit to the model equations at 13 different frequencies, allowing a precise determination of the model parameters. A series of ECIS measurements for five wells at 13 frequencies takes about ten minutes.

As an example of the measurement of cell-substrate separation, Fig. 2a and 2b show transcellular resistance and capacitance values as a function of frequency, for cell-free electrodes and for electrodes covered with a confluent layer of cells, measured at 37 °C. To get normalized values, we divide the impedance values of cell-covered electrodes by the corresponding quantities of the cell-free electrodes (Fig. 3). Using Eq. (1), the best fitting values of R_b and α are 0.28 GΩ μm^2 (2.8 Ω cm^2) and 60 Ω$^{1/2}$ mm. We calculate h from α by using Eq. (2) with $\rho = 540$ Ω mm and $r_c = 16$ μm. The result for the average cell-substrate separation at 37 °C is 38 nm.

Magnetic beads and force application

Ferric oxide beads (Fe_3O_4, Aldrich Chemicals, Milwaukee, Wisconsin) were coated with collagen by incubating 0.4 g of beads at 37 °C for one hour with 1 ml collagen solution (3 mg/ml; Vitrogen, Collagen Corp., Palo Alto, California), neutralized to pH 7.4 with 100 μl 1 N NaOH (Glogauer et al. 1995). Following washing of the beads and sonication to eliminate clumping, beads were added to dishes containing substrate-attached cells for ten minutes. The cell layer was then washed three times to remove un-

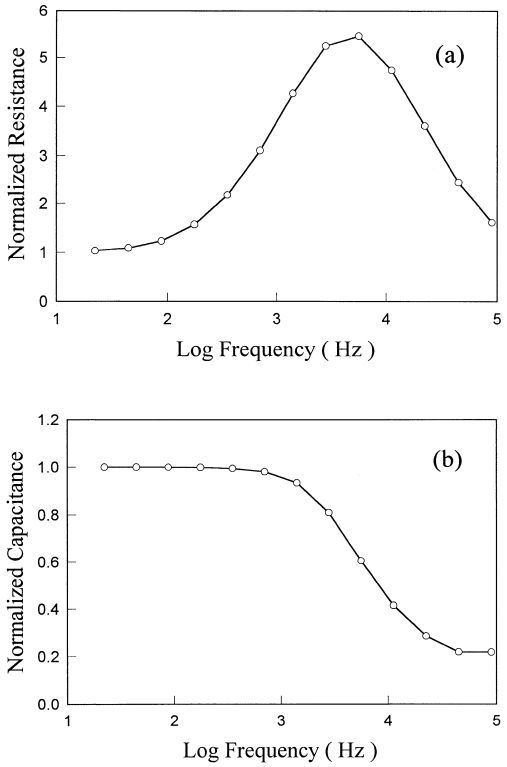

Fig. 3 **a** Normalized resistance and **b** normalized capacitance for an electrode with a confluent cell layer. The curves are obtained from Fig. 2 by dividing the measured values for the cell-covered electrode by the corresponding values for the cell-free electrode

bound beads. The collagen coated beads are bound by integrin receptors in the dorsal plasma membrane, and there is a clustering of attachment points of the cytoskeletal actin microfilaments to integrin receptors binding the beads (Glogauer et al. 1997). The force applied by the beads will thus be transmitted via the cytoskeleton to the integrin-ligand adhesion bonds that attach the cell to the plastic substrate of the culture dish.

The distribution of bead diameters was measured via electronic counting (Coulter Channelyzer, Coulter Electronics, Hialeah, Florida), and also by computer analysis of images obtained via a CCD camera with a phase contrast microscope (Optimas image analysis program, Optimas Corp., Bothell, Washington; PentaMAX CCD system, Princeton Instruments, Stittsville, Ontario; Nikon Optiphot microscope with 40× objective, Toronto, Ontario). This distribution was used to obtain number-weighted averages for bead diameter (2.5 μm), cross-sectional area (7.0 μm^2), and volume (21.0 μm^3).

A permanent magnet provided the magnetic field (Duramax 8, Dura Magnetics, Sylvania, Ohio). It had dimensions of 152×101×25 mm, with the larger surfaces being the pole faces. To apply an upward force to the dorsal surfaces of the cells, the center of a pole face was placed 20 mm above the cell layer. The magnetic force per unit volume of bead at this distance was directly measured by electronic balance, giving 0.21 pN μm^{-3}. Using mean bead volume and cross-sectional area, this can be converted to a force per unit area of bead coverage: 0.63 pN μm^{-2}. We used a bead coverage of 50% of the dorsal surface, with a resulting upward force per cell of 320 pN (3.2×10^{-5} dyne). This force is less than 10% of that found necessary to remove fibroblasts from a fibronectin covered substrate (Lotz et al. 1989), and it does not detach cells in our experiments. The applied force can be increased by a factor of 1.75 by using two magnets placed together (N pole face to S pole face) and placing the center of a pole face 20 mm from the cell layer.

Fluorescence measurements of cell ventral area

We carried out a series of fluorescence microscopy measurements of the cell ventral area after loading magnetic beads on the dorsal surface, with and without applied force. Cells were loaded with the fluorescent indicator calcein. Ventral area was obtained from computer analysis of digitized images obtained via a computer-controlled CCD television camera attached to a phase-contrast microscope (image analysis/CCD camera system as described above).

Results and discussion

Analysis of ECIS frequency scan measurements shows that the average separation between the ventral cell surface and substrate, h, increases from 38 to 45 to 84 nm as the temperature decreases from 37° to 22° to 4 °C (Table 1). There is also an increase in cell-to-cell junctional resistance with temperature, which is largely attributable to the temperature dependence of the extracellular medium resistivity. However, there seems to be some increase in distance between the cells upon going from 37° to 22 °C, since the cell-to-cell junctional resistance, R_b, does not increase as much as the medium resistivity, ρ.

The ventral surface of adherent cells is not perfectly flat (Izzard and Lochner 1976, 1980). Our results suggest that the topology of the ventral surface changes with temperature, with the area of close contact between cell and substrate decreasing as temperature decreases from 37° to 4°,

Table 1 Effect of temperature on cell-substrate separation

	ρ (Ω mm)	R_b (GΩ μm^2)	α ($\Omega^{1/2}$ mm)	h (nm)
37 °C (n=10)	540	0.28±0.01	60±1	38±2
22 °C (n=10)	700	0.29±0.01	63±1	45±2
4 °C (n=10)	1140	0.51±0.01	59±1	84±4

Two parameters are used to fit the measured cell layer impedance as a function of frequency: R_b, which is the junctional resistance between cells, and $\alpha(=r_c(\rho/h)^{1/2})$, where r_c is cell radius, ρ is extracellular medium resistivity, and h is average cell-substrate separation. The ± values are estimates based on both the reproducibility of the impedance measurements and the sensitivity of the model impedance curves to the parameters

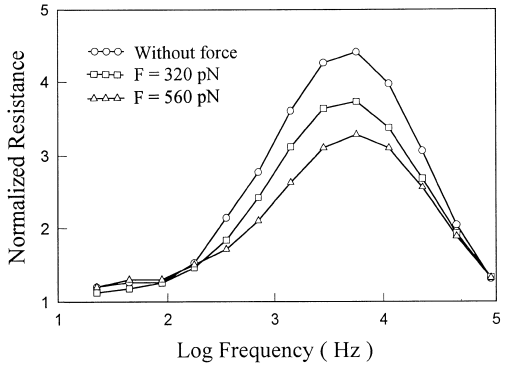

Fig. 4 Normalized resistance curves measured at 37 °C for a confluent cell layer with collagen-coated magnetic beads attached to the dorsal surfaces of the cells. The *upper curve* is with zero applied force (no magnet), the *middle curve* has an applied force of 320 pN per cell (one magnet), and the *lower curve* has 560 pN per cell (two magnets). The values of model parameters obtained from the ECIS analysis of these three curves are R_b (GΩ μm^2): 0.14, 0.07, 0.05 and α ($\Omega^{1/2}$ mm): 58, 55, 50 (upper, middle, and lower curves, respectively). The resulting *h* values are 41, 46 and 55 nm

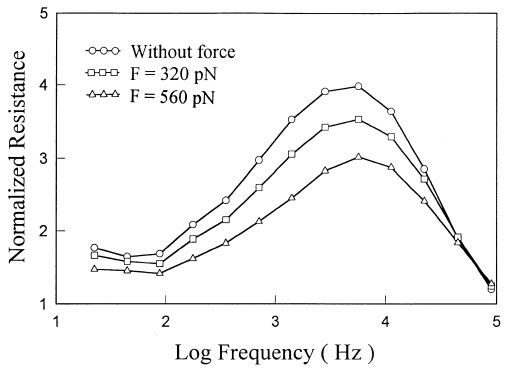

Fig. 5 Normalized resistance curves measured at 22°C for a confluent cell layer with collagen-coated magnetic beads attached to the dorsal surfaces of the cells. The *upper curve* is with zero applied force (no magnet), the *middle curve* has an applied force of 320 pN per cell (one magnet), and the *lower curve* has 560 pN per cell (two magnets). The values of model parameters obtained from the ECIS analysis of these three curves are R_b (GΩ μm^2): 0.23, 0.18, 0.13 and α ($\Omega^{1/2}$ mm): 50, 46, 43 (upper, middle, and lower curves, respectively). The resulting *h* values are 72, 85 and 97 nm

since the ECIS measurement for *h* gives the average separation of the ventral surface from the substrate, including the close contact areas as well as the areas that are not as close. This would agree with the results of Lotz et al. (1989), who showed in an interference reflection microscopy study of glioma cell adhesion to fibronectin that the focal contact area (with cell-substrate separation ≤15 nm) is less at 4° than at 37°.

After loading magnetic beads on the dorsal surface of the cells, we use ECIS frequency scan measurements to obtain the change in cell-substrate distance, Δ*h*, resulting from force applied via a permanent magnet placed 20 mm above the cells. Figures 4 and 5 show how the normalized resistance curve (normalized resistance vs. frequency)

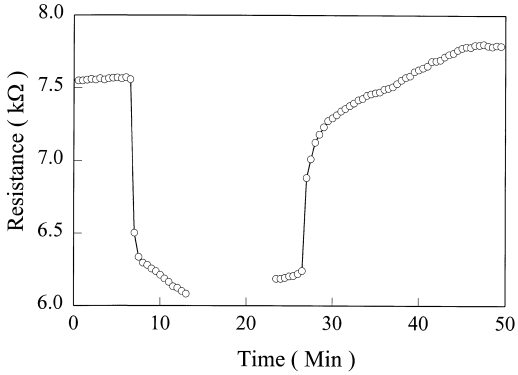

Fig. 6 Time course of measured resistance following initiation of force application (320 pN at 37°) and following termination of force application. These time courses show that there are rapid changes following a change in force, which are indicative of an elastic response, as well as slower changes suggestive of a viscoelastic response. In these measurements the resistance has two components, one being resistance to current flow beneath the cell layer, which depends on cell-substrate separation, and the other being resistance to current flow between the cells, which depends on cell-cell separation. To distinguish between these resistance components the frequency scan measurements must be used

changes in response to applied force. After each ECIS measurement with an applied force, the magnet is removed and the measurement repeated: at 37° there is reversal of the force-induced change in *h* in almost every measurement, at both force levels, with the frequency scan curves and the resulting *h* values being close to the pre-force values; at 22° there is usually reversal at 320 pN per cell, but most measurements at 560 pN per cell show incomplete recovery. Figures 4 and 5 also show that junctional resistance between the cells, R_b, decreases with applied force. This decrease implies that the cell-to-cell separation increases with applied force, but only of the order of tens of nanometers.

The measured electrical variables change too quickly following force application and force removal to allow a time course for *h* to be obtained via ECIS frequency scan measurements. However, we can carry out a simpler resistance vs. time measurement. We use a 1 μA injected current at a frequency of 4 kHz. This measures the sum of resistance to current flowing beneath the cells, and resistance to current flowing between the cells. These measurements show a time course with at least two time constants, suggesting that there are both elastic and viscoelastic processes at work (Fig. 6).

Our fluorescence measurements show that the ventral area of the cells changes little during application of 320 pN per cell: the 99% confidence interval for the ratio of ventral area measured before force application to that measured during force application, seven minutes after initial force application, is 0.993 to 1.008 ($n = 8$). Furthermore, this force is almost certainly not strong enough to cause significant distortion of the ventral surface topology, as shown by a calculation based on the elastic properties of actin filaments in the Appendix. With a constant topology, the change in cell-substrate separation would be

uniformly equal to our measured Δh over the entire ventral surface.

Another way to look at this is that, in the absence of dynamical peeling of the adhesion bonds (Ward and Hammer 1993), the force applied to the dorsal surface of the cell via the magnetic beads should be transmitted to all of the adhesion bonds on the ventral surface via the cytoskeleton. Even using a low estimate for the number of adhesion bonds, $N_{bond} \approx 10^3$ (Bell et al. 1984; Hammer and Laufenburger 1987; Ward and Hammer 1993; Ward et al. 1994, 1995), the applied force per bond, F ($=F_{cell}/N_{bond}$ =320 pN/10^3 = 0.3 pN), would be two orders of magnitude below the force required to break individual receptor-ligand bonds as measured by atomic force microscopy (at least 70 pN per iminobiotin-avidin bond; Florin et al. 1994). With $F_{cell} = 320$ pN at 37°, the potential energy increase resulting from stretching the integrin-adhesion molecule complex, given by $F_{cell}\Delta h/N_{bond}$, would be no greater than 1.6 pN nm (1.6×10^{-11} J), which is less than the average thermal energy per degree of freedom ($k_BT/2$). These low values for force and energy input per adhesion bond are a strong indication that our applied force is not causing significant ventral surface deformation.

To obtain the overall spring constant for cell-substrate binding, k_{cell}, we divide the applied force by Δh: $k_{cell} = F/\Delta h$ (Table 2). Our measured values for Δh are proportional to the applied force, giving the same k_{cell} for both force levels used. Under our conditions of measurement, in the presence of fetal bovine serum, adhesion should consist of integrin-fibronectin and integrin-vitronectin bonds (Preissner 1991; Hayashi 1993), and we have confirmed using an enzyme-linked immunosorbent assay (ELISA) that both fibronectin and vitronectin are present under our cells (unpublished data). A reasonable range of numbers for the adhesion bonds per cell is 10^3 to 10^5 (Bell et al. 1984; Hammer and Laufenburger 1987; Ward and Hammer 1993; Ward et al. 1994, 1995). Using these numbers for N_{bond}, our measured values for k_{cell} at 37° give a range for the spring constant of the individual adhesion bond, k_{bond} ($=k_{cell}/N_{bond}$), of from 6×10^{-4} to 6×10^{-2} pN nm^{-1} (dyne cm^{-1}). This range for k_{bond} overlaps the lower end of the ranges used in a number of mathematical models for cell adhesion (Bell et al. 1984; Dembo et al. 1988; Ward and Hammer 1993; Ward et al. 1994, 1995). The high end of our range is close to the "best estimate" of Bell et al. (1984) of 10^{-1} pN nm^{-1} (dyne cm^{-1}).

Theoretical estimates of k_{bond} vary widely, from 10^{-2} to 10^3 pN nm^{-1} (dyne cm^{-1}), with the lower values based on the assumption of a random coil, and the higher ones based on the properties of a rigid α-helix (Bell et al. 1984; Dembo et al. 1988; Ward and Hammer 1993). For a random coil, $k_{bond} = k_BT/h^2 \approx 4$ pN nm/h^2, where k_B is Boltzmann's constant and T is absolute temperature. Using our measured value at 37° of $h \approx 40$ nm, this gives a value of 2.5×10^{-3} pN nm^{-1}. Although fibronectin and vitronectin are not random coils, they contain a number of flexible regions that could impart a high degree of flexibility to the molecule as a whole. Moreover, the elastic properties of the cell-substrate bond will be influenced by forces generated by the numerous oligosaccharide chains attached to the cell surface, which are very flexible. Our values for k_{bond} thus may be describing the elastic properties of the integrin-adhesion molecule complex and its surrounding oligosaccharides.

The spring constant of most macromolecules would be expected to show little change upon going from 22° to 37°C. On the other hand, if this temperature increase would induce a melting-type phase transition, as from an α-helix to a random coil, this would lead to a dramatically reduced k_{bond}. Thus, in either case, our measurements showing that k_{cell} has an increase of approximately 100% upon going from 22° to 37° are evidence that N_{bond} increases with temperature. Thermodynamically, the integrin-ligand affinity should decrease as temperature increases (Hammer and Lauffenburger 1987; Ward and Hammer 1993), which would lead to a decrease in the steady state ratio of bound to unbound adhesion receptors as temperature increases. This means that the increase in N_{bond} with temperature that our measurements imply must involve active cellular processes rather than being a purely physicochemical effect.

In this paper we have reported the first direct measurement of the effect of an applied force on the cell-substrate distance. Our results provide values for the spring constant of the cell-substrate distance, and allow us to estimate the range of possible values for the spring constant of individual adhesion bonds. Our data also provide strong evidence that the number of adhesion bonds increases with temperature. Further development of the methods employed here should provide considerable insight into the mechanisms of cellular adhesion.

Table 2 Effect of force on cell-substrate separation

	F (pN)	Δh (nm)	k_{cell} (pN nm^{-1})
37 °C (n=5)	320	5±2	64 (46~107)
37 °C (n=5)	560	9±2	62 (51~ 80)
22 °C (n=5)	320	11±3	29 (23~ 40)
22 °C (n=5)	560	21±3	27 (23~ 31)

The change in cell-substrate separation, Δh, produced by the force applied via the magnetic beads, F, provides the overall spring constant for cellular adhesion, $k_{cell} = F/\Delta h$. The ± values for Δh are estimates based on the reproducibility of the force-induced shifts in the measured impedance curves, and the sensitivity of the model impedance curves to the parameters α and R_b (see Table 1)

Appendix: estimation of ventral surface distortion

In this appendix we present an approximate calculation for the distortion of the ventral surface of the cell that is induced by the applied force. In Fig. 7a we have a representation of the cell and its cytoskeleton. The integrin receptors on the dorsal surface that are binding magnetic beads are connected by actin filament bundles to points on the ventral surface of the cell, including both integrin recep-

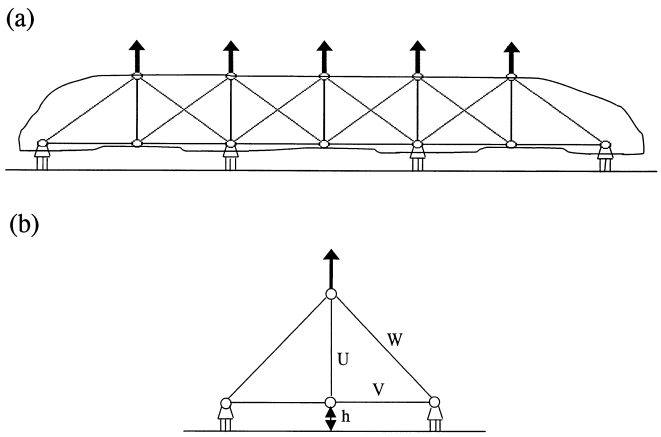

Fig. 7 **a** Represents a model for the vertical cross-section through a cell, showing points of force application on the dorsal surface where magnetic beads are bound to integrin receptor complexes (force is indicated by the *arrows*). Cytoskeletal elements (represented by the *vertical* and *diagonal lines*) connect these force application points to points on the ventral surface, where in some cases there are attachment bonds that link integrin receptors in the cell membrane to the substrate. We will assume that the diagonal elements are actin filament bundles, while the vertical elements could comprise microtubules and intermediate filaments as well as actin filaments. The ventral and dorsal surfaces will be strengthened by the cortex, comprising various elements of the cytoskeleton in a mesh-like structure; there could also be actin filaments running between the points on the ventral surface, and between the points on the dorsal surface. **b** Shows one unit of this structure

tors bound to extracellular attachment proteins, and integrins or other cell membrane bound proteins that are not attached to extracellular proteins. We can first consider a basic unit of this structure, comprising a single integrin receptor complex on the dorsal surface that is binding a magnetic bead, two ventral surface points of attachment to the substrate, and a point between these two attachment points where an actin filament bundle connects to the ventral membrane (Fig. 7b).

Note that in Fig. 7, the arrows indicate the applied magnetic force, but the geometry shown is for zero force. When force is applied, the points at which the actin filament bundles connect to the ventral membrane without a link via attachment proteins to the substrate will move upward relative to the points that have such links to the substrate, by an amount to be calculated below. This calculation is based on the effect of the applied force on the actin filament bundles, and of course does not include the stretching of the attachment bonds that link the cell to the substrate.

The equations for force balance for the system in Fig. 7b are:

$$2\,T_W\left(\frac{U}{W}\right)+T_U=F\,,$$

and

$$2\,T_V\left(\frac{\Delta h'}{V}\right)=T_U\,,$$

where T_W, T_U and T_V are tension in the actin filament bundles that have lengths W, U and V, the magnetic force applied to the magnetic bead is F, and $\Delta h'$ is the force-induced change in h (the substrate-ventral membrane distance midway between the points of attachment to the substrate) that results from an upward bending (distortion) of the ventral surface of the cell.

The equations for stretching of the actin filament bundles for the system in Fig. 7b are:

$$\Delta W=\frac{T_W}{k_W}\,,$$

$$\Delta U=\frac{T_U}{k_U}\,,$$

and

$$\Delta V=\frac{T_V}{k_V}\,,$$

where k_W, k_U and k_V are spring constants for the actin filament bundles. Each k will be equal to $(EA)/L$, where E is the Young's modulus of the actin filament, A is the cross sectional area of the total number of filaments in the bundle, and L is the length of the bundle. We can also write for each bundle: $k=(k_{unit\,length}N)/L$, where $k_{unit\,length}$ is the spring constant for unit length of one actin filament, and N is the number of filaments in the bundle. In addition to actin filament bundles, the ventral surface will be strengthened by the cortex, containing actin and other cytoskeletal elements, which has a mesh-like structure (Janmey 1991). However, the elastic properties of the ventral surface have less importance in these calculations than those of the vertical and diagonal elements, as seen in the derivation below, and in the results of the more detailed computer calculations shown below.

An important geometrical relationship is:

$$\Delta h'+\Delta U=\left(\frac{W}{U}\right)\Delta W\,.$$

Given that ΔU will be greater than zero for an upward force, this relationship shows that $\Delta h'$ must be less than $(W/U)\,\Delta W$ for an upward force.

Solving all of the above equations, it is straightforward to show that:

$$\Delta h'\le\left(\frac{W}{U}\right)^2\frac{F}{2\,k_W}\,.$$

If the vertical bundles of actin filaments are much thicker than the diagonal ones, then $k_U \gg k_W$, and this inequality comes close to being an equality. From the measurements of Nishizaka et al. (1995), in which an optical tweezer is used to apply force to a single actin filament bound to a heavy meromyosin molecule which is attached to a rigid substrate, a lower bound on the the spring constant of a 5 μm long single actin filament can be obtained. For a fully stretched filament, this value is 0.6 pN nm^{-1}. For a 1 μm filament length, this becomes 3 pN nm^{-1}. Using 100 as a

typical value for N in the diagonal bundles, and using $U \approx 1$ μm and $W \approx \sqrt{2}$ μm, this gives $k_W \approx 200$ pN nm^{-1}, and for a magnetic force per bead of 4 pN, we have $\Delta h' \leq 0.02$ nm.

Extending the system shown in Fig. 7b to three magnetic beads and three points on the ventral surface attached to the substrate, with two points between these attachment points where the actin filament bundles connect to the ventral membrane, a computer calculation (using the TRUSSD program by Hsieh and Mau, 1995) gives $\Delta h' \approx 0.02$ nm. This result is with $k_U = k_W = k_V$. Increasing k_U to $10 \times k_W$ in this calculation, decreases $\Delta h'$ by about 30% (because some of the diagonal bundles then have less affect on $\Delta h'$), while varying k_V from 10× greater than k_W to 10× less changes $\Delta h'$ by less than 20%. This computer calculation gives similar results when extended to the system shown in Fig. 7a.

The number of actin filaments per bundle is a variable that depends on many factors. In the extreme case of having only ten filaments per diagonal bundle, the values given above for $\Delta h'$ would be increased by a factor of 10. These values are still considerably smaller than our measured values for Δh, the increase in distance between substrate and ventral cell surface with applied force. Our measured Δh includes not only the distortion effect calculated here but the stretching of the bonds that attach the cell to the substrate. The calculations presented here thus show that the stretching of the attachment bonds resulting from our applied force is much greater than the distortion of the ventral cell membrane resulting from the same force.

References

Bell GI (1978) Models for the specific adhesion of cells to cells. Science 200:618–227

Bell GI, Dembo M, Bongrand P (1984) Cell adhesion: competition between nonspecific repulsion and specific bonding. Biophys J 45:1051–1064

Crick FHC, Hughes AFW (1950) The physical properties of cytoplasm: a study by means of the magnetic particle method. Exp Cell Res 1:37–80

Dembo M, Torney DC, Saxman K, Hammer D (1988) The reaction-limited kinetics of membrane-to-surface adhesion and detachment. Proc R Soc Lond B 234:55–83

Ferrier J, Ward-Kesthely A, Homble F, Ross S (1987) Further analysis of spontaneous membrane potential activity and the hyperpolarizing response to parathyroid hormone in osteoblastlike cells. J Cell Physiol 130:344–351

Ferrier J, Kesthely A, Lagan E, Richter C (1991) An experimental test of a model for repeated Ca^{2+} spikes in osteoblastic cells. Biochem Cell Biol 69:433–441

Florin E-L, Moy VT, Gaub HE (1994) Adhesion forces between individual ligand-receptor pairs. Science 264:415–417

Frangos JA, Huang TY, Clark CB (1996) Steady shear and step changes in shear stimulate endothelium via independent mechanisms. Biochem Biophys Res Commun 224:660–665

Giaever I, Keese CR (1984) Monitoring fibroblast behavior in tissue culture with an applied electric field. Proc Natl Acad Sci USA 81:3761–3764

Giaever I, Keese CR (1986) Use of electric fields to monitor the dynamical aspect of cell behavior in tissue culture. IEEE Trans Biomed Eng 33:242–247

Giaever I, Keese CR (1991) Micromotion of mammalian cells measured electrically. Proc Natl Acad Sci USA 88:7896–7900

Giaever I, Keese CR (1993a) A morphological biosensor for mammalian cells. Nature 366:591–592

Giaever I, Keese CR (1993b) Correction. Proc Natl Acad Sci USA 90:1634

Glogauer M, Ferrier J, McCulloch CAG (1995) Magnetic fields applied to collagen-coated ferric oxide beads induce stretch-activated Ca^{2+} flux in fibroblasts. Am J Physiol 269:C1093–C1104

Glogauer M, Arora P, Yao G, Sokholov I, Ferrier J, McCulloch CAG (1997) Calcium ions and tyrosine phosphorylation interact coordinately with actin to regulate cytoprotective responses to stretching. J Cell Sci 110:11–21

Gumbiner BM (1996) Cell adhesion: the molecular basis of tissue architecture and morphogenesis. Cell 84:345–357

Hammer DA, Lauffenburger DA (1987) A dynamical model for receptor-mediated cell adhesion to surfaces. Biophys J 52: 475–487

Hayashi M (1993) Vitronectin: from vertebrates to invertebrates. In: Preissner KT, Rosenblatt S, Kost C, Wegerhoff J, Mosher DF (eds) Biology of vitronectins and their receptors. Excerpta Medica, New York, pp 3–11

Hiramoto T (1969) Mechanical properties of the protoplasm of the sea urchin egg. Exp Cell Res 56:201–208

Hsieh Y-Y, Mau ST (1995) Elementary Theory of Structures. Prentice Hall, Englewood Cliffs, pp 115–118, 360–363

Hynes RO (1987) Integrins: a family of cell surface receptors. Cell 48:549–554

Hynes RO (1992) Integrins: versatility, modulation, and signaling in cell adhesion. Cell 69:11–25

Hynes RO, Lander AD (1992) Contact and adhesive specificities in the associations, migrations, and targeting of cells and axons. Cell 68:303–322

Ingber DE (1990) Fibronectin controls capillary endothelial cell growth by modulating cell shape. Proc Natl Acad Sci USA 87:3579–3583

Israelachvili J, Wennersrstöm H (1996) Role of hydration and water structure in biological and colloidal interactions. Nature 379: 219–225

Izzard CS, Lochner LR (1976) Cell-to-substrate contacts in living fibroblasts: an interference reflexion study with an evaluation of the technique. J Cell Sci 21:129–159

Izzard CS, Lochner LR (1980) Formation of cell-to-substrate contacts during fibroblast motility: An interference-reflexion study. J Cell Sci 42:81–116

Janmey PA (1991) Mechanical properties of cytoskeletal polymers. Curr Opin Cell Biol 2:4–11

Lauffenburger DA, Horwitz AF (1996) Cell migration: a physically integrated molecular process. Cell 84:359–369

Leckband DE, Schmitt F-J, Israelachvili JN, Knoll W (1994) Direct force measurements of specific and nonspecific protein interactions. Biochemistry 33:4611–4624

Leijendekker WJ, Passaquin AC, Metzinger L, Ruegg UT (1996) Regulation of cytosolic calcium in skeletal-muscle cells of the mdx mouse under conditions of stress. Brit J Pharmacol 118: 611–616

Lo C-M, Keese CR, Giaever I (1993) Monitoring motion of confluent cells in tissue culture. Exp Cell Res 204:102–109

Lo C-M, Keese CR, Giaever I (1995) Impedance analysis of MDCK cells measured by electric cell-substrate impedance sensing. Biophys J 69:2800–2807

Lotz MM, Burdsal CA, Erickson HP, McClay DR (1989) Cell adhesion to fibronectin and tenascin: quantitative measurements of initial binding and subsequent strengthening response. J Cell Biol 109:1795–1805

Majeska RJ, Rodan GA (1982) The effect of $1,25(OH)_2D_3$ on alkaline phosphatase in osteoblastic osteosarcoma cells. J Biol Chem 257:3362–3365

Mikuni-Takagaki Y, Suzuki Y, Kawase T, Saito S (1996) Distinct responses of different populations of bone cells to mechanical stress. Endocrinol 137:2028–2035

Nishizaka T, Miyata H, Yoshikawa H, Ishiwata S, Kinosita K Jr (1995) Unbinding force of a single motor molecule of muscle measured using optical tweazers. Nature 377:251–254

Preissner KT (1991) Structure and biologcal role of vitronectin. Annu Rev Cell Biol 7:275–310

Sanderson MJ, Charles AC, Dirksen ER (1990) Mechanical stimulation and intercellular communication increases intracellular Ca^{2+} in epithelial cells. Cell Regul 1:585–596

Tregear R, Oiwa K, Chaen S, Sugi H (1993) Relation between magneticall-applied force and velocity in beads coated with rabbit myosin, sliding on actin cables in Nitellopsis cells. J Musc Res Cell Motil 14:412–415

Wang N, Butler JP, Ingber DE (1993) Mechanotransduction across the cell surface and through the cytoskeleton. Science 260:1124–1127

Wang N, Ingber DE (1995) Probing transmembrane mechanical coupling and cytomechanics using magnetic twisting cytometry. Biochem Cell Biol 73:327–335

Ward MD, Hammer DA (1993) A theoretical analysis for the effect of focal contact formation on cell-substrate attachment strength. Biophys J 64:936–959

Ward MD, Dembo M, Hammer DA (1994) Kinetics of cell detachment: peeling of discrete receptor clusters. Biophys J 67:2522–2534

Ward MD, Dembo M, Hammer DA (1995) Kinetics of cell detachment: effect of ligand density. Ann Biomed Eng 23:322–331

Xia S-L, Ferrier J (1992) Propagation of a calcium pulse between osteoblastic cells. Biochem Biophys Res Commun 186:1212–1219